Featured Letter

Optimization of Potent and Selective Cyclohexyl Acid ERAP1 Inhibitors Using Structure- and Property-Based Drug Design

Ross P. Hryczanek,* Andrew S. Hackett, Paul Rowland, Chun-wa Chung, Máire A. Convery, Duncan S. Holmes, Jonathan P. Hutchinson, Semra Kitchen, Justyna Korczynska, Robert P. Law, Jonathan D. Lea, John Liddle, Richard Lonsdale, Margarete Neu, Leng Nickels, Alex Phillipou, James E. Rowedder, Jessica L. Schneck, Paul Scott-Stevens, Hester Sheehan, Chloe L. Tayler, Ioannis Temponeras, Christopher P. Tinworth, Ann L. Walker, Justyna Wojno-Picon, Robert J. Young, David M. Lindsay, and Efstratios Stratikos

Cite This: https://doi.org/10.1021/acsmedchemlett.4c00401

Read Online

ACCESS | Metrics & More | Article Recommendations | Supporting Information

ABSTRACT: Endoplasmic reticulum aminopeptidase 1 (ERAP1) cleaves the *N*-terminal amino acids of peptides, which can then bind onto major histocompatibility class I (MHC-I) molecules for presentation onto the cell surface, driving the activation of adaptive immune responses. In cancer, overtrimming of mature antigenic peptides can reduce cytotoxic T-cell responses, and ERAP1 can generate self-antigenic peptides which contribute to autoimmune cellular responses. Therefore, modulation of ERAP1 activity has potential therapeutic indications for cancer immunotherapy and in autoimmune disease. Herein we describe the hit-to-lead

ERAP1 pIC$_{50}$ = 5.5
LE/LLE = 0.31/3.9
Hit 1

structure/property optimization

ERAP1 pIC$_{50}$ = 8.6
LE/LLE = 0.41/5.6
13

optimization of a series of cyclohexyl acid ERAP1 inhibitors, found by X-ray crystallography to bind at an allosteric regulatory site. Structure-based drug design enabled a >1,000-fold increase in ERAP1 enzymatic and cellular activity, resulting in potent and selective tool molecules. For lead compound **7**, rat pharmacokinetic properties showed moderate unbound clearance and oral bioavailability, thus highlighting the promise of the series for further optimization.

KEYWORDS: ERAP1, immunotherapy, structure-based drug design, property-based drug design, ligand efficiency, lipophilic ligand efficiency, FEP
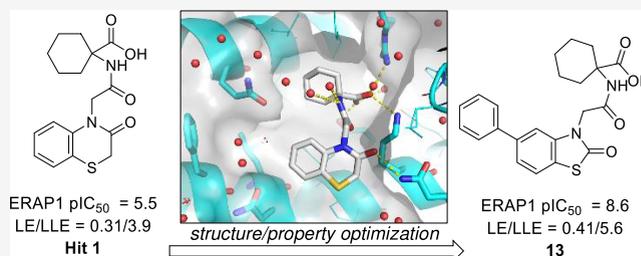
E ndoplasmic reticulum aminopeptidase 1 (ERAP1) cleaves *N*-terminal amino acids from antigenic peptide precursors for the downstream interaction with the adaptive immune system. Amino acids are sequentially cleaved from peptide lengths of up to 16 amino acid residues down to 8−10-mer peptides.[1] After trimming, these peptides are loaded onto MHC-I molecules, which are transported to the surface of the cell.[1−3] The complex composition of the antigenic peptides presented constitutes a representation of the state of the cell to the extracellular environment, which includes any potential malfunctions.[3] The peptide−MHC-I complexes are recognized by cells of the adaptive immune system response, such as cytotoxic T-cells, and this can induce apoptosis for infected or aberrant cells.[3]

Given that ERAP1-trimmed peptides modulate the adaptive immune response, controlling ERAP1 activity is an attractive strategy for cancer immunotherapy, autoimmune diseases and increasing immune responses against pathogens.[4] There is evidence of upregulation of ERAP1 in cancerous cells,[4] where peptides can be "overtrimmed" and thus cannot be presented in a complex with MHC-I, which has strict length require-

ments.[5] This effectively hides the cancerous cells from the immune system. Therefore, it is thought that inhibition of ERAP1 could prevent this "overtrimming" and thus highlight cancerous cells to the immune system that would have otherwise been hidden by up-regulated ERAP1.

A focus of developing ERAP1 modulators has been achieving selectivity over the closely related enzymes endoplasmic reticulum amino peptidase 2 (ERAP2) and insulin-regulated aminopeptidase (IRAP).[6−9] ERAP1, ERAP2 and IRAP have highly conserved active sites and around 50% sequence identities.[6] ERAP2 has a substrate preference different from that of ERAP1 but a similar function in regulating the adaptive immune response. IRAP also has a

A

Clerodane acid derivative[9]
ERAP1 pIC$_{50}$ = 6.0
HeLa cell antigen presentation pIC$_{50}$ = 5.7
ERAP2 pIC$_{50}$ <3.8
IRAP pIC$_{50}$ <3.6

Benzofuran hit[12]
ERAP1 pIC$_{50}$ = 6.4[a]
ERAP2 pIC$_{50}$ <4.5

Cyclohexyl acid hit compound 1
ERAP1 pIC$_{50}$ = 5.5
HeLa cell antigen presentation pIC$_{50}$ <4.3
ERAP2 pIC$_{50}$ <4.3[b]
IRAP pIC$_{50}$ <4.3[b]
LE / LLE = 0.31 / 3.9
ChromLogD$_{7.4}$ = 1.6
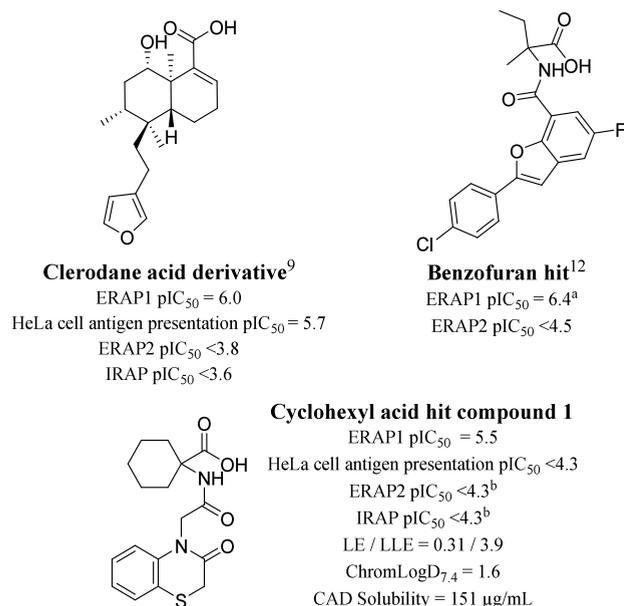CAD Solubility = 151 μg/mL

Figure 1. Profiling data for previously described clerodane acid derivative[9] and benzofuran hit.[12] This work describes the development of the cyclohexyl acid hit compound **1**. Peptidic substrates: ERAP1 (YTAFTIPSI or [a]L-Rho-Succ-FKARKF), HeLa cell antigen presentation (LEQLESIINFEKL), ERAP2 (Arg-AMC), IRAP (Leu-AMC). [b]n = 1.
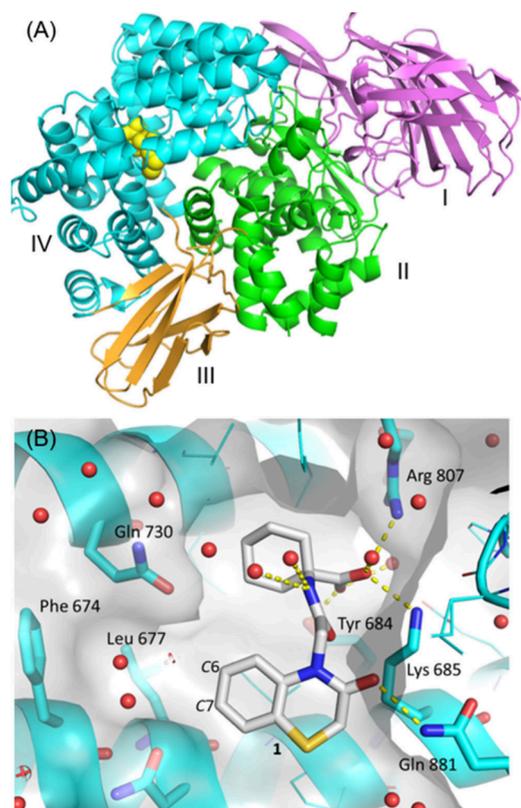

Figure 2. X-ray cocrystal structure of cyclohexyl acid compound **1** bound to ERAP1. Resolution 1.72 Å, PDB: 9GJN. (A) Compound **1** (yellow sphere), domain I (pink), domain II (green), domain III (gold), domain IV (cyan). (B) Compound **1** in binding site (gray)

similar function to ERAP1 and, additionally, regulates both glucose uptake into cells and oxytocin levels in pregnancy.[10]

Currently, there are no approved ERAP1 inhibitor therapeutics; therefore, there is a need to develop highly potent and selective inhibitors with good pharmacokinetic exposure.[11] Potent phosphinic pseudotripeptide ERAP1 inhibitors with limited ERAP2 and IRAP selectivity have been reported,[3,7] as have selective molecules with lower ERAP1 inhibition potency.[6,8,9] A series of benzofuran carboxylic acids with nanomolar potency were found to be selective over ERAP2 but were not tested against IRAP (Figure 1).[12] A series of phenyl-sulfamoyl benzoic acid inhibitors from Gray Wolf Therapeutics have been reported with nanomolar activity.[13] A compound from this series, GRWD5769, is currently in phase 1/2 clinical trials for patients with advanced solid tumors.[11]

Within our laboratories, the natural product clerodane acid derivative (Figure 1) was identified from a high-throughput screen for ERAP1 modulators.[9] This compound activates the hydrolysis of the small fluorogenic substrate Leu-AMC 2−2.5-fold yet inhibits the cleavage of antigenic epitope YTAFTIPSI (pIC$_{50}$ = 6.0). The clerodane acid derivative also showed excellent selectivity over ERAP2 and IRAP and was active in regulating the immunopeptidome of a melanoma cancer cell line.[14] We were encouraged by the clerodane acid derivative results but sought to develop alternative chemical matter with increased synthetic tractability. The objective was to find ERAP1 inhibitors, using physiologically relevant antigenic peptide substrates, working toward the "overtrimming" hypothesis, where it is thought that ERAP1 may destroy mature antigenic peptides of cancer cells.[4]

Also discovered in the same high-throughput screen as the clerodane acid derivative was the hit cyclohexyl acid compound **1**, which had ERAP1 inhibitory potency and a selectivity profile similar to those of the clerodane acid derivative (Figure 1). Hit compound **1** was found by X-ray crystallography to bind at the same regulatory site as the clerodane acid derivative (Figure 2). Compound **1** had reduced structural complexity compared to the clerodane acid derivative and was therefore considered a more synthetically tractable molecule for hit-to-lead optimization. The structure, efficiency, and physical properties of compound **1** represented an attractive starting point; the structure- and property-based optimization of compound **1** is the focus of this work.

Enzymatic ERAP1 activity was assessed using a high-throughput mass spectrometry assay that measures the cleavage of the 9-amino acid peptide YTAFTIPSI to form TAFTIPSI, as described previously.[9] This antigenic natural epitope precursor was derived from the human immunodeficiency virus[15] and was chosen as it is a highly ERAP1-sensitive substrate.[6] In this assay, compound **1** had an ERAP1 pIC$_{50}$ value of 5.5. Cellular activity was measured using a flow cytometry-based assay that measures the presentation of the antigenic epitope SIINFEKL,[9] and compound **1** did not show measurable inhibitory activity in this assay. Compound **1** has a ChromLogD$_{7.4}$[16] value of 1.6, and this low lipophilicity could result in poor cell membrane permeability, which could explain the lack of cellular activity.[17] Thus, in addition to increasing potency, a primary objective of this work was to increase the lipophilicity of hit compound **1** with the aim of achieving cellular potency. The charge and low lipophilicity of compound **1** resulted in high aqueous solubility based on a kinetic CAD measurement.[18,19]

Table 1. Early SAR Investigations of Systematic Point Changes to Hit 1 ERAP1 and Cell Potency (Data Are n = 3 or Higher unless Otherwise Stated)
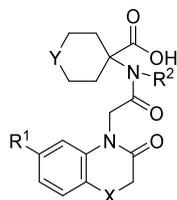
Cmd	R^1	R^2	X	Y	ERAP1 pIC_{50}	HeLa cell antigen presentation pIC_{50}	ChromLogD$_{7.4}$	LE	LLE	Aq. Sol. (μg/mL)
1	H	H	S	CH$_2$	5.5	<4.3	1.6	0.31	3.9	≥151
2	Cl	H	S	CH$_2$	6.7	NT	2.0	0.37	4.7	≥211
3	Cl	H	O	CH$_2$	7.1	5.4[a]	2.0	0.39	5.2	≥112
4	Br	H	O	CH$_2$	7.3	6.0[b]	2.0	0.40	5.3	≥172
5	CF$_3$	H	O	CH$_2$	7.3	6.0[c]	2.3	0.36	5.0	≥172
6	Br	H	O	S	7.9	6.3[b]	1.6	0.43	6.3	≥170
7	Br	H	O	CF$_2$	7.7	7.0	2.0	0.39	5.7	≥198
8	Br	Me	O	CH$_2$	7.3	6.3	2.5	0.38	4.9	80
9	Ph	H	O	CH$_2$	7.9	NT	2.7	0.36	5.2	≥228

[a]Tested at <4.3 on two test occasions. [b]n = 2. [c]Tested at <4.3 on one test occasion. NT = not tested
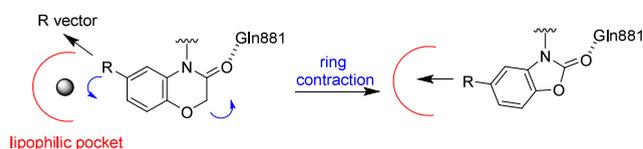

Figure 3. Schematic of the design hypothesis for 5,6-bicyclic systems.

We recognized the opportunity to increase lipophilicity but aimed to do this in a controlled and efficient manner, and therefore we proactively pursued increases in lipophilic ligand efficiency (LLE; Figure 1).[20] We used a variation of LLE defined as ERAP1 pIC_{50} − ChromLogD$_{7.4}$.[16] In addition, ligand efficiency (LE) was also tracked to ensure heavy-atom count was being used efficiently.[20] The benefits of optimizing LE and LLE have been discussed extensively[21−25] and include improved target selectivity, improved ADMET properties and greater design flexibility throughout optimization. Further,

marketed drug molecules tend to have superior LE and LLE values compared to published nondrug molecules.[20,25] For this work, specific target values for LE and LLE were not chosen; instead, the objective was to simply increase LE and LLE from their values in hit **1**. Ultimately, increasing potency in a lipophilicity and heavy-atom efficient manner should yield higher quality leads with greater lipophilicity and heavy-atom flexibility for any potential future lead optimization.

Three major binding interactions were observed from the carboxylic acid of compound **1** to Arg807, Lys685 and Tyr684 (Figure 2). These key interactions are thought to be where the C-termini of endogenous peptides bind.[26] Binding of peptides to the regulatory site plays a critical role in determining ERAP1 substrate length requirements and the extent to which peptide trimming occurs through a "molecular ruler" mechanism.[2] The cyclohexane ring occupied a lipophilic pocket, and the attached amide did not clearly show any specific polar interactions with

Table 2. SAR Investigations of 5,6-Bicyclic Systems (ERAP1 and Cell Potency Data Are n = 3 or Higher unless Otherwise Stated)
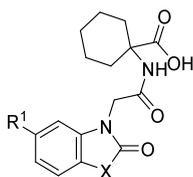
Cmd	R^1	X	ERAP1 pIC_{50}	HeLa cell antigen presentation pIC_{50}	ChromLogD$_{7.4}$	LE	LLE	Aq. Sol. (μg/mL)
10	Br	O	6.6	NT	1.9	0.38	4.7	≥194
11	Ph	O	8.1[a]	6.7[b]	2.8	0.38	5.3	≥157
12	Ph	CH$_2$	8.2	6.7[c]	2.6	0.39	5.6	≥165
13	Ph	S	8.6[d]	7.7	3.0	0.41	5.6	112
14	(cyclohexyl)	S	8.2	7.0	3.9	0.39	4.3	≥127

[a]Tested >8.8 on one test occasion. [b]Tested <4.3 on two test occasions. [c]n = 2. [d]Tested >8.8 on two test occasions. NT = not tested.
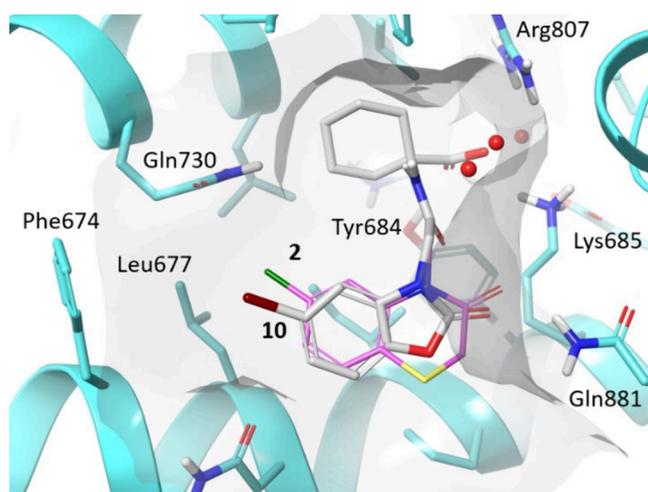
C

Figure 4. X-ray cocrystal structure of compound **2** (ligand pink, protein blue, resolution 1.33 Å, PDB: 9GK6), overlaid with docked pose of compound **10** (gray) used in FEP simulations.
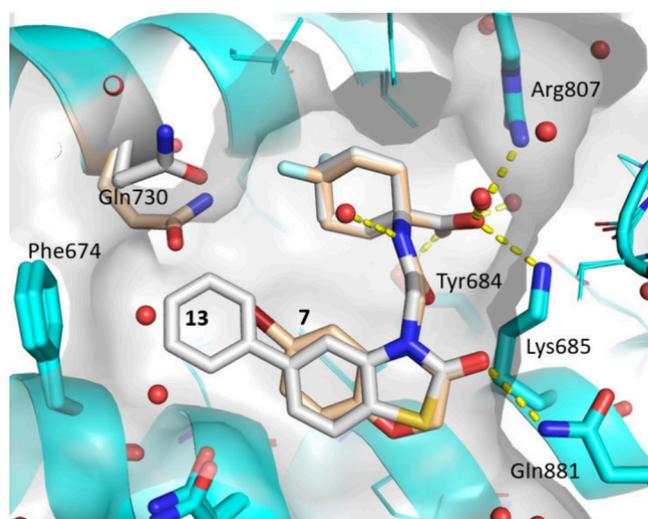

Figure 5. X-ray cocrystal structure overlay of compound **7** (beige, 1.35 Å resolution, PDB: 9GJS) and compound **13** (gray, 1.37 Å resolution, PDB: 9GKE) bound to ERAP1 (cyan). Significant movement in Gln730 was observed between the binding of compounds **7** and **13**.

the protein. An additional hydrogen bond interaction was observed from the carbonyl of the thiomorpholinone motif with Gln881. Adjacent to the aromatic ring of the benzothiomorpholinone was a pocket containing lipophilic residues Phe674 and Leu677, shown to be occupied by a water molecule. Previously reported benzofuran compounds that contained examples featuring the same cyclohexyl acid-amide motif were predicted by docking studies to have similar binding, though they did not make the hydrogen-bonding interaction with Gln881.[12]

Based on the binding of compound **1**, molecules with systematic single-atom point changes were designed and synthesized (Table 1), with the aim of increasing ERAP1 potency and potentially achieving cellular activity by the introduction of lipophilic motifs. The first area investigated was the substitution of the bicyclic motif, as the X-ray cocrystal structure indicated potential space for growth into the lipophilic pocket containing Phe674 and Leu677 (Figure 2).
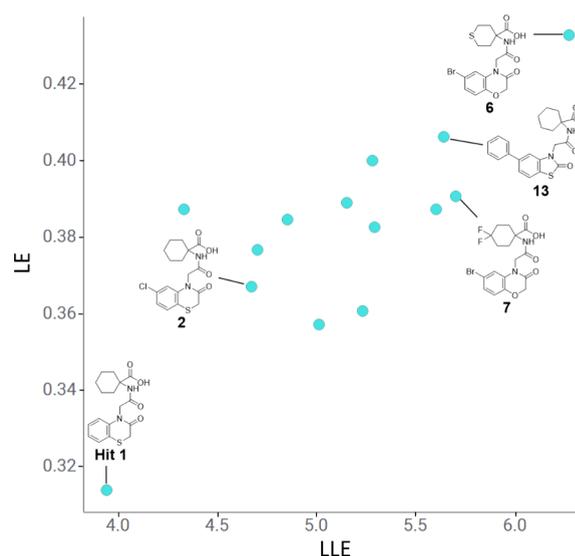

Figure 6. LE and LLE progress from hit **1**.

The C6 and C7 positions of the benzothiomorpholinone ring did not appear as ideal vectors to grow into this space; however, it was hypothesized that if movement in the protein and ligand was tolerated, then this substitution may increase ERAP1 potency.

Halogenation of the C6 position resulted in chloro-substituted compound **2**, which was over 10-fold more potent compared to the hit compound **1** in the enzymatic assay. Subsequently, the thiomorpholinone motif was investigated, with exchange of the sulfur atom for an oxygen also leading to increased potency, as shown by morpholinone **3**. Alternative lipophilic substitutions at the C6 position of the benzothiomorpholinone motif, such as bromide derivative **4** and trifluoromethyl analogue **5**, were well tolerated. Modified cyclohexane rings, such as sulfide **6** and difluorocyclohexane **7**, resulted in further increases in potency. Methylation of the amide, giving compound **8**, was potency neutral compared to the N−H matched pair **4**, which was somewhat expected, given that the N−H did not appear to make any specific interactions with the protein and pointed toward solvent in the X-ray crystal structure. This change did, however, increase lipophilicity and remove a hydrogen bond donor, and therefore it was considered a useful physicochemical property modulation handle. Finally, phenyl-substituted compound **9** demonstrated that large lipophilic groups were well tolerated, suggesting significant movement in the binding site or ligand. Without significant movement of the protein or ligand, a large phenyl ring would result in clashes with Gln730 (Figure 2).

As shown in Table 1, compounds **2**−**9** had improved LE and LLE values compared to hit compound **1**, indicating that potency had been improved in a heavy-atom and lipophilicity efficient manner. Despite the increases in lipophilicity, high aqueous solubility was maintained for all compounds, with a slight reduction for tertiary amide **8**, where a hydrogen bond donor had been removed.

Cell potency was achieved for optimized compounds shown in Table 1, although the differences between enzymatic and cellular potency were not consistent for the compounds. For example, **3** and **7** had 1.7 and 0.7 log unit differences, respectively, despite having the same lipophilicity. These results suggest that lipophilicity-dependent permeability is

D

Table 3. *In Vitro* Clearance and *In Vivo* Rat PK Data for Compounds 7 and 13

		IV			PO				*In vitro* Hepatocyte CL_{int} (mL/min/g tissue)			
Cmd	Dose IV/PO (mg/kg)	$V_{d,ss}$ (L/kg)	$CL/CL_u{}^{a}$ (mL/min/kg)	$T_{1/2}$(h)	C_{max} (ng/mL)	AUC_{0-t} (ng·h/mL)	Rat $F_{u,blood}$	%F	Human	Rat	FaSSIF sol. 4 h (µg/mL)	Caco-2 Papp (AP/BL) (nm/s)
7	1.0/2.6	4.0	39.0/283	3.6	67.1	229	0.138	18	0.52	0.63	>1,000	48
13	1.0/2.0	2.1	79.6/7236	0.98	8.0	10.0	0.011	3	1.97	5.44	58	30

$^{a}CL_u$ = unbound *in vivo* clearance, calculated by dividing intravenous clearance (IV CL) by $F_{u,blood}$.

likely not the sole reason for the differences in biochemical and cellular activity. The ERAP1 gene is polymorphic, resulting in several ERAP1 allotypes being present in human populations, which differ in their enzymatic activity, antigen presentation and sensitivity to allosteric inhibition.[26] We used the Hap2 construct for the isolated enzyme assay;[9] however, 74% of the population do not express this haplotype.[26] Polymorphic variation could contribute to the inconsistent differences in activity between the purified Hap2 construct used in the biochemical assay and the effects on antigen presentation in HeLa cells. Further, the two assays used different peptide substrates; again, this could contribute to inconsistencies in activity between compounds. Despite these considerations, we were encouraged that high potency was achieved in the ERAP1 biochemical and cellular antigen presentation assays for the cyclohexyl acid series.

A variety of point changes of hit compound **1** had resulted in >100-fold increases in potency. Additional X-ray crystal structures were obtained, including chloro compound **2** (see Figure 4). It was clear from the X-ray crystal structure that the lipophilic pocket containing Phe674 and Leu677 was not efficiently filled by the chlorine atom. In our next phase of design, we therefore questioned whether we could increase potency further by filling the lipophilic pocket more efficiently using our structural knowledge. We thus turned to free energy perturbation (FEP) simulations as a tool to prioritize ideas for synthesis.[27] Several design ideas were predicted using FEP, including a ring contraction of the 6,6-bicyclic motif to a 5,6-bicyclic motif (Figure 3). The hypothesis here was to maintain the hydrogen bond to Gln881, which should act as an anchor, allowing the bicyclic system to rotate and offer a more direct vector to explore the lipophilic pocket.

From the ideas scored and prioritized using binding affinity predictions from the FEP simulations, oxazolidinone **10**, containing a 5,6-bicyclic ring system, had a predicted ERAP1 pIC_{50} of 6.2. When synthesized and tested, this translated into a measured pIC_{50} of 6.6 (Table 2). The binding pose of compound **10** generated for FEP is shown in Figure 4, overlaid with the X-ray crystal structure of compound **2**, which was used as the FEP reference structure. Consistent with our design hypothesis, the structures depicted in Figure 4 suggest a more direct R vector for the Br substituent into the lipophilic pocket compared with the 6,6-bicyclic compound **2**. Based on this modeling, it was thought that the Br atom of compound **10** was not large enough to efficiently fill the lipophilic pocket. Introduction of the larger phenyl motif at R^1, in compound **11**, resulted in a significantly increased enzymatic pIC_{50} value of 8.1 (Table 2).

We then designed further analogues containing 5,6-bicyclic motifs, compounds **12** to **14** (Table 2). Indolinone **12** showed similarly high ERAP1 potency to **11**, and the sulfur variant **13**

led to a further increase in enzymatic ERAP1 pIC_{50} to 8.6, and one of the highest LLE values in this set. Nonaromatic alternatives were also well tolerated, as demonstrated by cyclohexyl derivative **14**. With respect to hit compound **1**, the 5,6-bicyclic compounds achieved the objectives of increasing LE and LLE while maintaining high aqueous solubility.

Additional X-ray cocrystal structures of several cyclohexyl acid series compounds were solved, with the aim of understanding the differences in binding between the 6,6- and 5,6-bicyclic systems (Figure 5). The binding modes of compound **7** (ERAP1 pIC_{50} = 7.7) and compound **13** (ERAP1 pIC_{50} = 8.6) largely overlaid well. As predicted for the FEP pose for compound **10**, the most significant difference was in the orientation of the bicyclic ring, which presented the bromine atom and phenyl ring of compounds **7** and **13**, respectively, into the lipophilic pocket. Comparing the two structures, there was also a significant movement of Gln730 to better fit the size and orientation of the ligand. Notably, a range of bicyclic systems, with both small and large substituents, were able to achieve high potency, with significant movement in the pocket observed to accommodate the ligand.

Both LE and LLE were actively monitored throughout SAR exploration, and these parameters were increased significantly from hit compound **1** (Figure 6). Optimization of LE was pursued by investigating systematic single-point changes without significantly increasing heavy-atom count, for example, in aryl chloride **2**. For LLE, this parameter was optimized by targeting the lipophilic pocket containing Phe674 and Leu677. The objective here was that any increases in potency should be from specific ERAP1 interactions rather than nonspecific lipophilicity-driven binding. These strategies resulted in significant increases in both LE and LLE during optimization. Compound **6** was particularly efficient with the highest LE and LLE values; however, the molecule had significantly lower cellular activity compared to other cyclohexyl acid series compounds.

Given that the cyclohexyl acid series now contained highly potent ERAP1 inhibitors, we sought to understand whether selectivity over ERAP2 and IRAP had been retained from the hit compound **1**. To examine this selectivity, we tested compound **7**, which was one of the most potent compounds in both the biochemical and cellular assays at the time. Selectivity was measured as described previously, by determining pIC_{50} values for hydrolysis of small fluorogenic substrates Arg-AMC or Leu-AMC for ERAP2 and IRAP, respectively.[9] Pleasingly, **7** showed no measurable inhibition of ERAP2 or IRAP (pIC_{50} < 4.0, n = 1) and thus had >1,000-fold ERAP1 selectivity. Selectivity was also observed with the natural product clerodane acid derivative, which was found to bind at the same regulatory site as compound **1** (Figure 1).[9] Further, docking of structurally related benzofuran compounds, which

are selective over ERAP2, indicated binding at the same allosteric site.[12] This evidence supports the hypothesis that ERAP2 and IRAP do not have the same allosteric regulatory binding site as ERAP1.[28,29] This binding site hypothesis, in addition to the selectivity data for compounds **1** and **7**, gives us confidence that the potential therapeutic benefits of the cyclohexyl acid series could be tested without potential complications arising from interactions with ERAP2 and IRAP.

Given the progress made in enzymatic and cellular potency for the cyclohexyl acids, we evaluated examples from the series in rat *in vivo* PK studies (Table 3). Compound **13** had a high unbound intravenous clearance and poor oral exposure in rat. However, given the high cellular pIC_{50} value of 7.7, this molecule would potentially be suitable as an *in vitro* tool. In contrast, compound **7** had a significantly reduced unbound *in vivo* clearance with both good oral exposure and bioavailability. Furthermore, compound **7** demonstrated a much lower *in vitro* intrinsic clearance in rat and human hepatocytes, is 10-fold less lipophilic than compound **13**, and has a much higher FaSSIF solubility. Taken together, this may explain, in part, the difference in oral bioavailability between compound **7** and compound **13**. Following the expected lipophilicity trend,[27] the more polar compound **7** had a higher fraction unbound value in rat blood. The volume of distribution for both compounds was surprisingly high, where carboxylic acids typically have volume of distribution values between 0.1 and 0.4 L/kg.[30] Both compounds had moderate permeabilities in the Caco-2 permeability assay. Given the encouraging *in vivo* PK results of compound **7**, the cyclohexyl acid series was considered a promising series for lead optimization.

In conclusion, a series of ERAP1 inhibitors have been developed, examples of which have >1,000-fold increased potency over hit cyclohexyl acid **1**. High potency in the HeLa cell antigen presentation assay was also achieved, with the most potent example, **13**, displaying a pIC_{50} of 7.7. Optimization focused on a combination of systematic single-atom point changes and structure-based drug design supported by FEP potency predictions. X-ray crystallography confirmed that the 5,6-bicyclic motifs accessed the lipophilic pocket formed by Phe674 and Leu677 more directly compared to the 6,6-bicyclic systems. As part of the optimization, active pursuit and tracking of LE and LLE efficiency metrics resulted in simultaneous increases in both of these parameters. Both hit compound **1** and lead compound **7** were found to be selective over ERAP2 and IRAP. Furthermore, compound **7** had promising pharmacokinetic properties in rats, providing an excellent starting point for further optimization, which will be the subject of future publications.

Safety Statement. No unexpected safety observations were noted from this work. Novel compounds were assumed toxic as a precaution.

■ ASSOCIATED CONTENT

Data Availability Statement

The coordinates and structure factors have been deposited in the Protein Data Bank under the accession codes 9GJN (**1**), 9GK6 (**2**), 9GJS (**7**), and 9GKE (**13**).

ⓢ Supporting Information

The Supporting Information is available free of charge at https://pubs.acs.org/doi/10.1021/acsmedchemlett.4c00401.

Compound synthesis and characterization, LCMS and NMR traces for key compounds, assay standard deviations and replicates, assay methods, X-ray crystallography methods, FEP methods (PDF)

■ AUTHOR INFORMATION

Corresponding Author

Ross P. Hryczanek — *GSK, Medicines Research Centre, Stevenage SG1 2NY, U.K.; Department of Pure and Applied Chemistry, University of Strathclyde, Glasgow G1 1XL, U.K.;* ⓞ orcid.org/0009-0003-7005-4477; Email: ross.p.hryczanek@gsk.com

Authors

Andrew S. Hackett — *GSK, Medicines Research Centre, Stevenage SG1 2NY, U.K.*

Paul Rowland — *GSK, Medicines Research Centre, Stevenage SG1 2NY, U.K.*

Chun-wa Chung — *GSK, Medicines Research Centre, Stevenage SG1 2NY, U.K.;* ⓞ orcid.org/0000-0002-2480-3110

Máire A. Convery — *GSK, Medicines Research Centre, Stevenage SG1 2NY, U.K.*

Duncan S. Holmes — *GSK, Medicines Research Centre, Stevenage SG1 2NY, U.K.*

Jonathan P. Hutchinson — *GSK, Medicines Research Centre, Stevenage SG1 2NY, U.K.*

Semra Kitchen — *GSK, Medicines Research Centre, Stevenage SG1 2NY, U.K.*

Justyna Korczynska — *GSK, Medicines Research Centre, Stevenage SG1 2NY, U.K.*

Robert P. Law — *GSK, Medicines Research Centre, Stevenage SG1 2NY, U.K.;* ⓞ orcid.org/0000-0002-2585-4585

Jonathan D. Lea — *GSK, Medicines Research Centre, Stevenage SG1 2NY, U.K.*

John Liddle — *GSK, Medicines Research Centre, Stevenage SG1 2NY, U.K.*

Richard Lonsdale — *GSK, Medicines Research Centre, Stevenage SG1 2NY, U.K.;* ⓞ orcid.org/0000-0001-9160-4659

Margarete Neu — *GSK, Medicines Research Centre, Stevenage SG1 2NY, U.K.*

Leng Nickels — *GSK, Medicines Research Centre, Stevenage SG1 2NY, U.K.*

Alex Phillipou — *GSK, Medicines Research Centre, Stevenage SG1 2NY, U.K.*

James E. Rowedder — *GSK, Medicines Research Centre, Stevenage SG1 2NY, U.K.*

Jessica L. Schneck — *GSK, Medicines Research Centre, Stevenage SG1 2NY, U.K.*

Paul Scott-Stevens — *GSK, Medicines Research Centre, Stevenage SG1 2NY, U.K.*

Hester Sheehan — *GSK, Medicines Research Centre, Stevenage SG1 2NY, U.K.*

Chloe L. Tayler — *GSK, Medicines Research Centre, Stevenage SG1 2NY, U.K.*

Ioannis Temponeras — *National Center for Scientific Research "Demokritos", Attiki 15341, Greece*

Christopher P. Tinworth — *GSK, Medicines Research Centre, Stevenage SG1 2NY, U.K.;* ⓞ orcid.org/0000-0002-2756-707X

Ann L. Walker — *GSK, Medicines Research Centre, Stevenage SG1 2NY, U.K.*

Justyna Wojno-Picon — *GSK, Medicines Research Centre, Stevenage SG1 2NY, U.K.*

Robert J. Young − *GSK, Medicines Research Centre, Stevenage SG1 2NY, U.K.;* ● orcid.org/0000-0002-7763-0575

David M. Lindsay − *Department of Pure and Applied Chemistry, University of Strathclyde, Glasgow G1 1XL, U.K.;* ● orcid.org/0000-0003-4498-5094

Efstratios Stratikos − *National Center for Scientific Research "Demokritos", Attiki 15341, Greece;* ● orcid.org/0000-0002-3566-2309

Notes

The authors declare the following competing financial interest(s): All authors except I. T., E. S. and D. M. L. are current or former employees of GSK. J. L. is currently an employee of AstraZeneca. I. T. is currently an employee of Protavio. J. W.-P. is currently an employee of Evotec. R. J. Y. is currently principal of Blue Burgundy.

Human biological samples were sourced ethically, and their research use was in accord with the terms of the informed consents under an IRB/REC approved protocol. All animal studies were ethically reviewed and carried out in accordance with Animals (Scientific Procedures) Act 1986 and the GSK Policy on the Care, Welfare, and Treatment of Animals.

■ ABBREVIATIONS

ADMET, absorption, distribution, metabolism, excretion, toxicity; CAD, charged aerosol detection; ERAP2, endoplasmic reticulum amino peptidase 2; FEP, free energy perturbation; IRAP, insulin-regulated aminopeptidase; LE, ligand efficiency; LLE, lipophilic ligand efficiency; MHC-I, major histocompatibility class I; PK, pharmacokinetics; SAR, structure−activity relationship

■ REFERENCES

(1) Stratikos, E.; Stern, L. J. Antigenic Peptide Trimming by ER Aminopeptidases - Insights from Structural Studies. *Mol. Immunol.* **2013**, *55* (3−4), 212−219.

(2) Gandhi, A.; Lakshminarasimhan, D.; Sun, Y.; Guo, H.-C. Structural Insights Into the Molecular Ruler Mechanism of the Endoplasmic Reticulum Aminopeptidase ERAP1. *Sci. Rep.* **2011**, *1*, 186.

(3) Zervoudi, E.; Saridakis, E.; Birtley, J. R.; Seregin, S. S.; Reeves, E.; Kokkala, P.; Aldhamen, Y. A.; Amalfitano, A.; Mavridis, I. M.; James, E.; Georgiadis, D.; Stratikos, E. Rationally Designed Inhibitor Targeting Antigen-Trimming Aminopeptidases Enhances Antigen Presentation and Cytotoxic T-Cell Responses. *Proc. Natl. Acad. Sci. U.S.A.* **2013**, *110* (49), 19890−19895.

(4) Babaie, F.; Hosseinzadeh, R.; Ebrazeh, M.; Seyfizadeh, N.; Aslani, S.; Salimi, S.; Hemmatzadeh, M.; Azizi, G.; Jadidi-Niaragh, F.; Mohammadi, H. The Roles of ERAP1 and ERAP2 in Autoimmunity and Cancer Immunity: New insights and Perspective. *Mol. Immunol.* **2020**, *121*, 7−19.

(5) Evnouchidou, I.; van Endert, P. Peptide Trimming by Endoplasmic Reticulum Aminopeptidases: Role of MHC Class I Binding and ERAP Dimerization. *Hum. Immunol.* **2019**, *80* (5), 290−295.

(6) Stamogiannos, A.; Papakyriakou, A.; Mauvais, F.-X.; van Endert, P.; Stratikos, E. Screening Identifies Thimerosal as a Selective Inhibitor of Endoplasmic Reticulum Aminopeptidase 1. *ACS Med. Chem. Lett.* **2016**, *7* (7), 681−685.

(7) Kokkala, P.; Mpakali, A.; Mauvais, F.-X.; Papakyriakou, A.; Daskalaki, I.; Petropoulou, I.; Kavvalou, S.; Papathanasopoulou, M.; Agrotis, S.; Fonsou, T.-M.; van Endert, P.; Stratikos, E.; Georgiadis, D. Optimization and Structure-Activity Relationships of Phosphinic Pseudotripeptide Inhibitors of Aminopeptidases That Generate Antigenic Peptides. *J. Med. Chem.* **2016**, *59* (19), 9107−9123.

(8) Maben, Z.; Arya, R.; Rane, D.; An, W. F.; Metkar, S.; Hickey, M.; Bender, S.; Ali, A.; Nguyen, T. T.; Evnouchidou, I.; Schilling, R.; Stratikos, E.; Golden, J.; Stern, L. J. Discovery of Selective Inhibitors of Endoplasmic Reticulum Aminopeptidase 1. *J. Med. Chem.* **2020**, *63* (1), 103−121.

(9) Liddle, J.; Hutchinson, J. P.; Kitchen, S.; Rowland, P.; Neu, M.; Cecconie, T.; Holmes, D. S.; Jones, E.; Korczynska, J.; Koumantou, D.; Lea, J. D.; Nickels, L.; Pemberton, M.; Phillipou, A.; Schneck, J. L.; Sheehan, H.; Tinworth, C. P.; Uings, I.; Wojno-Picon, J.; Young, R. J.; Stratikos, E. Targeting the Regulatory Site of ER Amino-peptidase 1 Leads to the Discovery of a Natural Product Modulator of Antigen Presentation. *J. Med. Chem.* **2020**, *63* (6), 3348−3358.

(10) Georgiadis, D.; Ziotopoulou, A.; Kaloumenou, E.; Lelis, A.; Papasava, A. The Discovery of Insulin-Regulated Aminopeptidase (IRAP) Inhibitors: A Literature Review. *Front. Pharmacol.* **2020**, *11*, 585838.

(11) Fougiaxis, V.; He, B.; Khan, T.; Vatinel, R.; Koutroumpa, N. M.; Afantitis, A.; Lesire, L.; Sierocki, P.; Deprez, B.; Deprez-Poulain, R. ERAP Inhibitors in Autoimmunity and Immuno-Oncology: Medicinal Chemistry Insights. *J. Med. Chem.* **2024**, *67* (14), 11597−11621.

(12) Deddouche-Grass, S.; Andouche, C.; Bärenz, F.; Halter, C.; Hohwald, A.; Lebrun, L.; Membré, N.; Morales, R.; Muzet, N.; Poirot, M.; Reynaud, M.; Roujean, V.; Weber, F.; Zimmermann, A.; Heng, R.; Basse, N. Discovery and Optimization of a Series of Benzofuran Selective ERAP1 Inhibitors: Biochemical and In Silico Studies. *ACS Med. Chem. Lett.* **2021**, *12* (7), 1137−1142.

(13) Quibell, M.; Shiers, J. J.; Sparenberg, M. ERAP1 Modulators. World Patent WO2021094763A1, 2021.

(14) Temponeras, I.; Samiotaki, M.; Koumantou, D.; Nikopaschou, M.; Kuiper, J. J. W.; Panayotou, G.; Stratikos, E. Distinct Modulation of Cellular Immunopeptidome by the Allosteric Regulatory Site of ER Aminopeptidase 1. *Eur. J. Immunol.* **2023**, *53* (8), 2350449.

(15) Shankar, P.; Russo, M.; Harnisch, B.; Patterson, M.; Skolnik, P.; Lieberman, J. Impaired Function of Circulating HIV-Specific CD8+ T Cells in Chronic Human Immunodeficiency Virus Infection. *Blood* **2000**, *96* (9), 3094−3101.

(16) Valkó, K.; Bevan, C.; Reynolds, D. Chromatographic Hydrophobicity Index by Fast-Gradient RP-HPLC: A High-Throughput Alternative to log P/log D. *Anal. Chem.* **1997**, *69* (11), 2022−2029.

(17) Young, R. J.; Green, D. V. S.; Luscombe, C. N.; Hill, A. P. Getting Physical in Drug Discovery II: the Impact of Chromato-graphic Hydrophobicity Measurements and Aromaticity. *Drug Discovery Today* **2011**, *16* (17), 822−830.

(18) Robinson, M. W.; Hill, A. P.; Readshaw, S. A.; Hollerton, J. C.; Upton, R. J.; Lynn, S. M.; Besley, S. C.; Boughtflower, B. J. Use of Calculated Physicochemical Properties to Enhance Quantitative Response When Using Charged Aerosol Detection. *Anal. Chem.* **2017**, *89* (3), 1772−1777.

(19) Hill, A. P.; Young, R. J. Getting Physical in Drug Discovery: a Contemporary Perspective on Solubility and Hydrophobicity. *Drug Discovery Today* **2010**, *15* (15), 648−655.

(20) Hopkins, A. L.; Keserü, G. M.; Leeson, P. D.; Rees, D. C.; Reynolds, C. H. The Role of Ligand Efficiency Metrics in Drug Discovery. *Nat. Rev. Drug Discovery* **2014**, *13*, 105.

(21) Freeman-Cook, K. D.; Hoffman, R. L.; Johnson, T. W. Lipophilic Efficiency: the Most Important Efficiency Metric in Medicinal Chemistry. *Future Med. Chem.* **2013**, *5* (2), 113−115.

(22) Scott, J. S.; Waring, M. J. Practical Application of Ligand Efficiency Metrics in Lead Optimisation. *Biorg. Med. Chem.* **2018**, *26* (11), 3006−3015.

(23) Johnson, T. W.; Gallego, R. A.; Edwards, M. P. Lipophilic Efficiency as an Important Metric in Drug Design. *J. Med. Chem.* **2018**, *61* (15), 6401−6420.

(24) Hann, M. M. Molecular Obesity, Potency and Other Addictions in Drug Discovery. *MedChemComm* **2011**, *2* (5), 349−355.

(25) Young, R. J.; Leeson, P. D. Mapping the Efficiency and Physicochemical Trajectories of Successful Optimizations. *J. Med. Chem.* **2018**, *61* (15), 6421−6467.

(26) Hutchinson, J. P.; Temponeras, I.; Kuiper, J.; Cortes, A.; Korczynska, J.; Kitchen, S.; Stratikos, E. Common allotypes of ER aminopeptidase 1 have substrate-dependent and highly variable enzymatic properties. *J. Biol. Chem.* **2021**, *296*, 100443.

(27) Watanabe, R.; Esaki, T.; Kawashima, H.; Natsume-Kitatani, Y.; Nagao, C.; Ohashi, R.; Mizuguchi, K. Predicting Fraction Unbound in Human Plasma from Chemical Structure: Improved Accuracy in the Low Value Ranges. *Mol. Pharmaceutics* **2018**, *15* (11), 5302−5311.

(28) Mpakali, A.; Giastas, P.; Mathioudakis, N.; Mavridis, I. M.; Saridakis, E.; Stratikos, E. Structural Basis for Antigenic Peptide Recognition and Processing by Endoplasmic Reticulum (ER) Aminopeptidase 2. *J. Biol. Chem.* **2015**, *290* (43), 26021−26032.

(29) Mpakali, A.; Saridakis, E.; Harlos, K.; Zhao, Y.; Papakyriakou, A.; Kokkala, P.; Georgiadis, D.; Stratikos, E. Crystal Structure of Insulin-Regulated Aminopeptidase with Bound Substrate Analogue Provides Insight on Antigenic Epitope Precursor Recognition and Processing. *J. Immunol.* **2015**, *195* (6), 2842−2851.

(30) Smith, D. A.; Beaumont, K.; Maurer, T. S.; Di, L. Clearance in Drug Design. *J. Med. Chem.* **2019**, *62* (5), 2245−2255.